Eurasian Journal of Physics and Functional Materials

Volume 9 | Number 3

Article 3

Pages: 1 - 1

2025

Development of Sr, Y, and Zn co-doped Ba0.3Ce0.7Zr0.1O3-δ dense electrolyte for intermediate temperature solid oxide fuel cell

Md. Mosfiqur Rahman
Faculty of Integrated Technologies, Universiti Brunei Darussalam, Gadong, BE1410, Brunei, mosfiqurju35@gmail.com

Jebun Naher Sikta
Industrial Physics Division, BCSIR Dhaka Laboratories, Bangladesh Council of Scientific and Industrial Research (BCSIR), Dhaka 1205, Bangladesh

Muhammed Ali
Fuel Cell Institute, Universiti Kebangsaan Malaysia, 43600 UKM Bangi, Selangor, Malaysia

Lukman Ahmed Omeiza
Faculty of Integrated Technologies, Universiti Brunei Darussalam, Gadong, BE1410, Brunei

Suravi Islam
Industrial Physics Division, BCSIR Dhaka Laboratories, Bangladesh Council of Scientific and Industrial Research (BCSIR), Dhaka 1205, Bangladesh

Recommended Citation

Rahman, Md. Mosfiqur; Sikta, Jebun Naher; Ali, Muhammed; Omeiza, Lukman Ahmed; Islam, Suravi; Wei, Bo; and Azad, Abul Kalam (2025) "Development of Sr, Y, and Zn co-doped Ba0.3Ce0.7Zr0.1O3-δ dense electrolyte for intermediate temperature solid oxide fuel cell," *Eurasian Journal of Physics and Functional Materials*: Vol. 9: No. 3, Article 3.
DOI: https://doi.org/10.69912/2616-8537.1254

Development of Sr, Y, and Zn co-doped Ba0.3Ce0.7Zr0.1O3-δ dense electrolyte for intermediate temperature solid oxide fuel cell

Authors

Md. Mosfiqur Rahman, Jebun Naher Sikta, Muhammed Ali, Lukman Ahmed Omeiza, Suravi Islam, Bo Wei, and Abul Kalam Azad

ORIGINAL STUDY

Development of Sr, Y, and Zn Co-doped $Ba_{0.3}Ce_{0.7}Zr_{0.1}O_{3-\delta}$ Dense Electrolyte for Intermediate Temperature Solid Oxide Fuel Cell

Md. M. Rahman [a,b,*], Jebun N. Sikta [c], Muhammed Ali [d], Lukman A. Omeiza [a], Suravi Islam [c], Bo Wei [e], Abul K. Azad [a,**]

[a] Faculty of Integrated Technologies, Universiti Brunei Darussalam, Gadong, BE1410, Brunei
[b] Faculty of Science & Information Technology, Daffodil International University, Dhaka 1341, Bangladesh
[c] Industrial Physics Division, BCSIR Dhaka Laboratories, Bangladesh Council of Scientific and Industrial Research (BCSIR), Dhaka 1205, Bangladesh
[d] Fuel Cell Institute, Universiti Kebangsaan Malaysia, UKM Bangi, 43600, Selangor, Malaysia
[e] School of Physics, Harbin Institute of Technology, Harbin, Heilongjiang 150001, China

Abstract

Polycrystalline perovskite-type $Ba_{0.3}Sr_{0.7}Ce_{0.7}Zr_{0.1}Y_{0.15}Zn_{0.05}O_{3-\delta}$ was synthesized and characterized by modifying two fundamental perovskites of $BaCeO_3$ and $BaZrO_3$. Solid state reaction (SSR) method was adopted for synthesizing the material. The traditional techniques such as X-ray diffraction (XRD), scanning electron microscopy (SEM), thermogravimetric analysis (TGA) and electrochemical impedance spectroscopy (EIS) were employed for the characterization. XRD analysis revealed its pure phase with cubic symmetry at 1300 °C sintering temperature. It was found to have high relative density by the Rietveld refinement process. Regarding thermal stability, it remained stable up to 800 °C. This material also posed crack-free surface. However, $Ba_{0.3}Sr_{0.7}Ce_{0.7}Zr_{0.1}Y_{0.15}Zn_{0.05}O_{3-\delta}$ provided relatively low activation energy with conductivity of 1.056×10^{-4} Scm^{-1} at 700 °C in air atmosphere. Therefore, the material might be used as a promising electrolyte in intermediate temperature solid oxide fuel cell (IT-SOFC).

Keywords: IT-SOFC, Electrolyte, Perovskite, Rietveld refinement, EIS

1. Introduction

In the last few decades, solid oxide fuel cell (SOFC) has become one of the most popular electrochemical energy conversion devices in the renewable energy sector. This is because SOFC environmental friendly and produces low emissions [1]. It converts the electrochemical energy into electric current by oxidizing fuel supplied in the anode [2]. Yttria-stabilized zirconia (YSZ) is usually used as electrolyte for the oxide-ion based SOFC (O-SOFC), which operates at high temperatures (800−1000 °C). The high temperatures used in O-SOFC result in cell degradation, a high fabrication cost and so on [3]. But the intermediate temperature solid oxide fuel cell (IT-SOFC), which normally operates at 600−800 °C [4,5], has some advantages over the O-SOFC. This is because proton-conducting electrolyte is used in IT-SOFC. Although proton-conducting solid oxide fuel cell offers higher efficiency than their oxide ion-conducting counterparts, they typically exhibit less power density and maximum voltage [6]. One of the most effective proton conductors is doped $BaCeO_3$; however, it lacks stability in the environments containing of H_2O and CO_2. This limitation can be addressed through appropriate doping. For instance, $BaZrO_3$—particularly when doped with 10 mole % yttrium—exhibits excellent stability in H_2O and CO_2 atmospheres, although its proton conductivity is

Received 23 June 2025; revised 30 July 2025; accepted 1 August 2025.
Available online 7 October 2025

* Corresponding author at: Faculty of Integrated Technologies, Universiti Brunei Darussalam, Gadong, BE1410, Brunei.
** Corresponding author.
E-mail addresses: mosfiqurju35@gmail.com (Md.M. Rahman), abul.azad@ubd.edu.bn (A.K. Azad).

https://doi.org/10.69912/2616-8537.1254

lower than that of $BaCeO_3$. Thus, the choice of dopant plays a crucial role in determining the material's electrical performance. Owing to their favorable stability and high proton conductivity in humid conditions, both $BaCeO_3$ and $BaZrO_3$ have attracted significant interest as base materials for doping [3,7]. Recently, $La_{0.9-x}Ba_xSr_{0.1}Ga_{0.8}Mg_{0.2}O_{3-\delta}$ (x = 0−0.08) electrolytes have been synthesized to examine the impact of Ba doping on structural and electrical properties. Doping with 5 mol % Ba improved structural stability, increased free volume by 4.1 %, and enhanced both bulk and grain boundary conductivities [8]. A series of $Ba_{1-x}Sr_xCe_{0.7}Zr_{0.1}Y_{0.15}Zn_{0.05}O_{3-\delta}$ (x = 0.1, 0.3, 0.5) compositions were studied, combining doped $BaCeO_3$ and $BaZrO_3$. X-ray diffraction showed peak shifts due to reduced unit cell volume with increasing Sr content. BSCZYZn (x = 0.1) had the highest ionic conductivity of 30.3×10^{-4} Scm^{-1} at 973 K and the lowest activation energy of 0.381 eV [9]. Ba-based proton-conducting $BaCe_{0.5}Zr_{0.3}Y_{0.1}A_{0.05}Zn_{0.05}O_{3-\delta}$ (A = Gd, Sm) electrolytes were synthesized for IT-SOFC applications. Electrochemical analysis showed that BCZYGdZn had significantly higher ionic conductivity than BCZYSmZn, with 12.9×10^{-4} Scm^{-1} in wet H_2 at 973 K and an activation energy of 0.38 eV. Both materials showed potential as electrolytes for IT-SOFC [10].

A study [11] introduces Ba diffusion sintering as an effective method to improve the densification and microstructure of $BaZr_{0.8}Yb_{0.2}O_{3-\delta}$ electrolyte for proton-conducting fuel cells. The incorporation of $BaCO_3$ at the anode, coupled with optimized sintering processes, results in improved grain growth and a uniform microstructure, effectively doubling the proton conductivity. An investigation [12] addresses the high sintering temperature requirement of the proton-conducting electrolyte $BaZr_{0.4}Ce_{0.4}Y_{0.1}Yb_{0.1}O_{2.9}$ (BZCYYb4411) by exploring three strategies to reduce it to 1400 °C: (1) ZnO addition, (2) Zn doping, and (3) fluorite-phase ZCYYb4411 addition. Zn-based methods proved most effective, achieving >90 % relative density and eliminating the need for a separate calcination step. The optimized samples showed high conductivity, with Zn-doped BZCYYb reaching 0.9×10^{-2} Scm^{-1} and ZnO-added BZCYYb reaching 0.6×10^{-2} Scm^{-1} at 700 °C in humidified N_2, demonstrating improved sintering and maintained performance. A new proton-conducting electrolyte $BaCe_{0.5}Zr_{0.3}Y_{0.1}Yb_{0.05}Zn_{0.05}O_{3-\delta}$ was introduced [13], designed for IT-SOFCs (400−700 °C). It was synthesized via solid-state reaction at 1400 °C, the material achieved 98 % density and exhibited an orthorhombic structure. It showed high chemical stability and protonic conductivity, with greater conductivity and lower activation energy in wet hydrogen. A single cell using this electrolyte and a BSCF cathode reached a peak power density of 649 $mWcm^{-2}$ at 973 K, highlighting its potential for practical SOFC applications. $BaCe_{0.9-x}In_xGd_{0.1}O_{3-\delta}$ (x = 0.1−0.4) electrolytes were synthesized via solid-state reaction method. Electrochemical tests showed that $BaCe_{0.6}In_{0.3}Gd_{0.1}O_{3-\delta}$ has stable cubic perovskite structure, over 97 % density, and excellent chemical stability in air. It achieved the highest conductivity (7.24 $mScm^{-1}$ at 873 K in dry H_2), making it a strong candidate for IT-SOFC electrolytes [14]. Fluorine doping (0−10 mol %) in $La_{0.9}Sr_{0.1}Ga_{0.8}Mg_{0.2}O_{3-\delta}$ significantly enhances ionic conductivity, achieving 3.8 $mScm^{-1}$ at 600 °C for 10 % F-doped samples. The result highlighted fluorine doping as a promising strategy for improving IT-SOFC electrolytes [15].

In this investigation, Sr was co-doped with Ba in the A-site, and Y, Zn were co-doped with Ce and Zr in the B-site of ABO_3 structure to understand the impact of dopants in making $Ba_{0.3}Sr_{0.7}$ $Ce_{0.7}Zr_{0.1}Y_{0.15}Zn_{0.05}O_{3-\delta}$ (BSCZYZn70) electrolyte for the possible application in IT-SOFC. Solid state reaction (SSR) technique was used to synthesize the material. Moreover, X-ray diffraction, scanning electron microscopy (SEM), thermogravimetric analysis (TGA), and electrochemical impedance spectroscopy (EIS) techniques were used to characterize the material.

2. Methodology

2.1. Synthesis

The material $Ba_{0.3}Sr_{0.7}Ce_{0.7}Zr_{0.1}Y_{0.15}Zn_{0.05}O_{3-\delta}$ (BSCZYZn70) was synthesized using the solid-state reaction method. Stoichiometric amounts of $SrCO_3$, $BaCO_3$, CeO_2, ZrO_2, Y_2O_3, and ZnO (provided by the company Sigma Aldrich) were precisely measured with an electronic analytical balance. These powders were mixed with acetone and ground in an agate mortar for about an hour, then calcined in air at 1000 °C for 8 h in a muffle furnace. The calcined powders were reground with acetone for another hour, pelletized into 13 mm under 5 tons of pressure, and sintered at 1300 °C for 12 h. In this study, Zn was added to enhance densification and lower the sintering temperature of the material [28,29]. To minimize impurities from unreacted oxides or carbonates, careful mixing was performed. To avoid any impurity or undesired peaks in the XRD patterns, the material usually reground and sintered again at higher temperatures for improving phase purity [16].

2.2. Characterizations of the material

Using a Shimadzu-7000 X-ray diffractometer ($CuK\alpha_1$ radiation, λ = 1.5406 Å), X-ray diffraction patterns were recorded over a 2θ range of 5°−80° with a step

size of 0.02° per minute at ambient temperature to investigate the structural properties of the mixed oxide material. The Rietveld refinement was utilized to examine the diffraction data [17]. The thermal behavior was analyzed utilizing Mettler Toledo (USA) apparatus over a temperature spectrum of 30–1200 °C, with heating and cooling rates of 10 °C/min. Microscopic characteristics were analyzed via a fourth-generation NeoScope JCM-7000. EIS was executed with the Admiral Squidstat Plus at open circuit voltage across a frequency spectrum of 200 kHz to 0.1 Hz, with a signal amplitude of 10 mV. BSCZYZn70 pellet was sintered, polished, and uniformly coated with platinum paste utilizing a Quorum Q150RS sputter coater to create a Pt/BSCZYZn70/Pt structure. The pellet measured around 13 mm in diameter and 4 mm in thickness, with a 6 mm-wide platinum-coated region on either side that functioned as the current collector. Impedance measurements were conducted in the air atmosphere across a temperature range of 500–800 °C, in 50 °C increments, with a heating rate of 3 °C/min. The sample was let to attain thermal equilibrium at each temperature prior to measurements. The impedance measurements were analyzed with Z-View software, employing the brick-layer model to elucidate the electrical behavior.

3. Results & discussion

3.1. Structural analysis

Fig. 1 displays the X-ray diffraction pattern of BSCZYZn70. FullProf and Checkcell software were used to reveal the indexing of BSCZYZn70 [9]. The indexing pattern was crystallized in cubic symmetry within *Pm-3m* space group. The most intense (highest) diffraction 2θ peak was observed in the range of 29–30°, while the least intense (lowest) 2θ peak appeared in the range of 76–80°. Fig. 2 displays the Rietveld profile of BSCZYZn70. The obtained parameters from the Rietveld refinement are represented by Table 1. The Rietveld refinement also confirmed the cubic symmetry and *Pm-3m* space group. The phase and space group of BSCZYZn70 can be compared to $BaCeO_3$ [18] and $BaZrO_3$ [19]. The crystal phase of $BaCeO_3$ and $BaZrO_3$ depends largely on the B-site composition, specifically the Ce and Zr content. Yttrium-doped $BaCeO_3$ typically exhibits an orthorhombic structure, while yttrium-doped $BaZrO_3$ tends to be cubic. In $BaCe_{0.9-x}Zr_xY_{0.1}O_{3-\delta}$, the phase remains orthorhombic for $x = 0.1$ to 0.2 and turns cubic for $x > 0.3$ [20]. For $BaCe_{0.8-x}Zr_xY_{0.2}O_{3-\delta}$, the structure is orthorhombic when $x = 0.1$ to 0.5 and becomes cubic at $x = 0.6$–0.8 [16]. The small difference in ionic radii between Y^{3+} (0.90 Å) and Zn^{2+} (0.74 Å) allows both to occupy the B-site without disrupting cubic symmetry. However, crystal symmetry can be significantly affected by factors like sintering temperature and synthesis method. Additionally, Ba^{2+} (1.61 Å) has a larger ionic radius than Sr^{2+} (1.44 Å) in the A-site, influencing the lattice structure [9]. As per Vegard's law, the noticed lattice parameter of BSCZYZn70 was 4.3022 Å. The theoretical density (from Rietveld analysis) and empirical density (by Archimedes' principle) of BSCZYZn70 were 5.721 gm/cm^3 and 5.720 gm/cm^3, respectively. Hence, the high relative density of 99.983 % indicates the

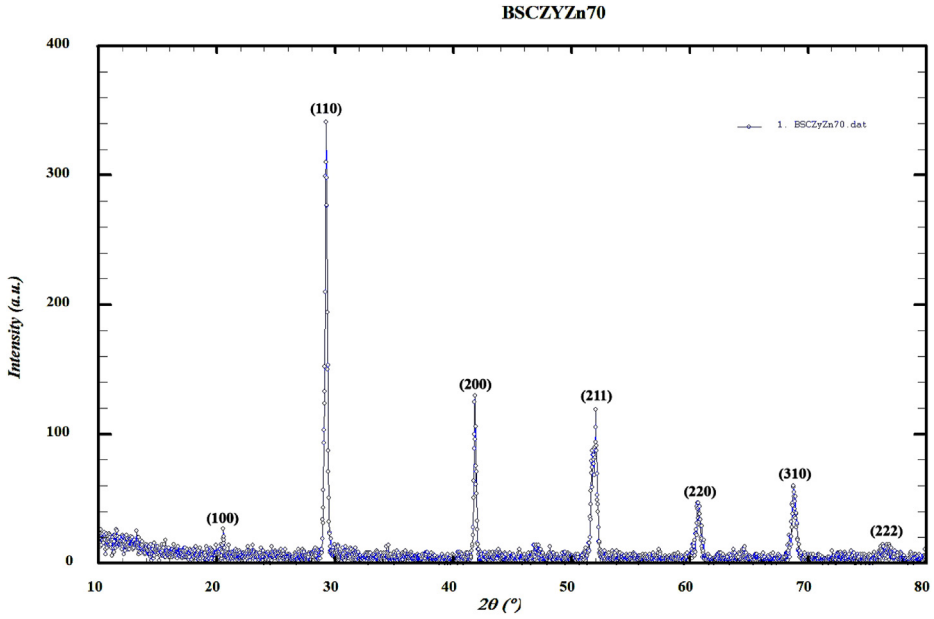

Fig. 1. X-ray diffraction pattern of BSCZYZn70.

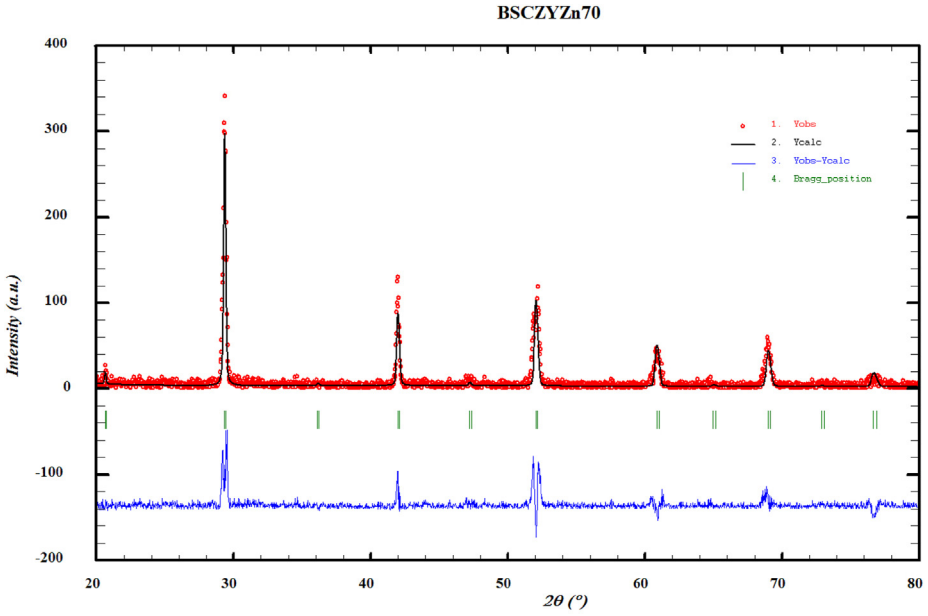

(a) Rietveld profile patterns of the XRD data of BSCZYZn70

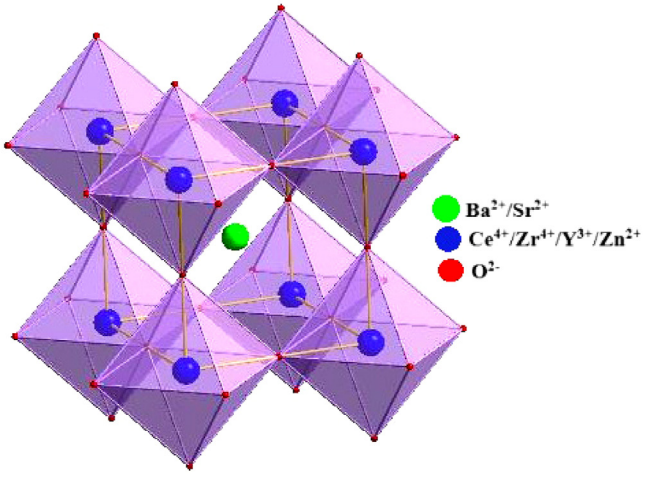

(b) 3D structure

Fig. 2. ***(a)*** *Rietveld profile patterns of the XRD data of BSCZYZn70* ***(b)*** *3D structure of BSCZYZn70.*

material has enhanced reactivity. However, the value of goodness-fit-parameter (χ^2 = 1.68), derived from Rietveld analysis, indicates the strong agreement between observed and calculated diffraction data.

3.2. Microstructure analysis

Fig. 3 describes the microscopic images of BSCZYZn70. The pellet surface of BSCZYZn70 was utilized to capture the images. The captured images were chosen with (a1) 10000X (a2) 5000X and (a3) 2500X magnifications. Since the electrolyte in SOFC must be gas-tight to prevent the mixing of gaseous reactants, analyzing the microstructure of the electrolyte material is necessity. One key factor affecting ionic conductivity is grain boundary resistance. In proton-conducting SOFC, larger grain sizes reduce the density of grain boundaries, thereby lowering grain boundary

Table 1. Rietveld refinement parameters of BSCZYZn70.

Sample	Lattice parameter a = b = c (Å)	Cell volume (Å^3)	χ^2	R_p	R_{wp}	R_e	$\rho_{theoretical}$ (g/cm^3)	$\rho_{empirical}$ (g/cm^3)	$\rho_{relative}$ (%)
BSCZYZn70	4.3022	79.628	1.68	30.8	41.9	32.3	5.721	5.720	99.983

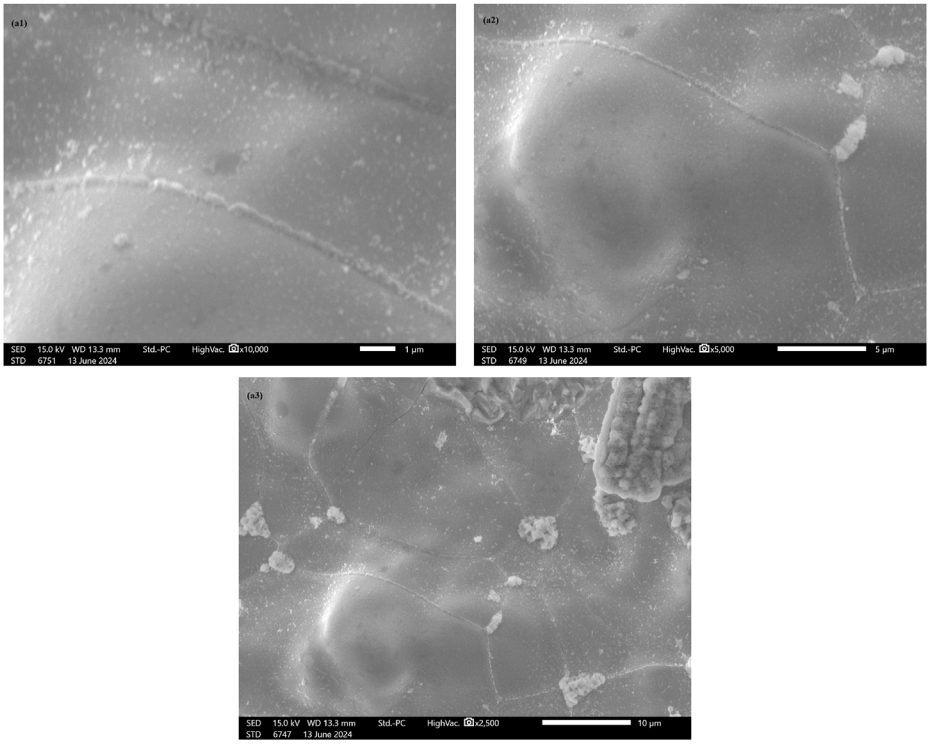

Fig. 3. Microscopic images of BSCZYZn70.

resistance and enhancing total ionic conductivity. In this study, the microstructural analysis reveals a highly dense structure with numerous well-defined grain boundaries. These boundaries, having high surface energy, facilitate effective ion transport toward the electrode, which is beneficial for SOFC performance [21–23]. High-resolution imaging confirms beneficial growth of grain, showing a variety of large and small grains with a dense surface morphology. Importantly, no liquid or secondary phases are detected at the grain boundaries, indicating a well-sintered and phase-pure material. The obtained result from this study can be compared to the previous studies [9,13,28,29]. Elemental distribution of BSCZYZn70 (represented by Table 2) using EDX further supports the material's integrity. The measured elemental ratios closely match the theoretical values derived from the chemical formula, with no evidence of unreacted or impurity phases, suggesting high material purity and successful synthesis. Whatsoever, the surface connectivity appears excellent, with no visible cracks or discontinuities. This intact microstructure enables efficient ion transport across the electrolyte, making the material a promising candidate for IT-SOFC.

Table 2. Elemental distribution of BSCZYZn70.

Sample	BSCZYZn70			
	Formula		EDX	
Element	Weight (%)	Atomic (%)	Weight (%)	Atomic (%)
Ba	18.45	15	17.80	14.88
Sr	27.45	35	29.07	38.10
Ce	43.90	35	45.91	37.63
Zr	4.08	5	4.12	5.18
Y	5.97	7.5	2.69	3.48
Zn	0.15	2.5	0.42	0.73

3.3. Thermal analysis

Fig. 4 displays the thermal weight loss of BSCZYZn70 in air atmosphere. A thorough understanding of the thermal stability and decomposition behavior of perovskite materials is substantive for their investigation. Thermogravimetric analysis plays an important role in this process, as it allows precise measurement of weight changes in perovskite samples. These measurements provide valuable insights into how the materials degrade when exposed to increasing temperatures. In this case, thermogravimetric measurement was taken under the temperature range of 30–1000 °C. The observed thermal loss was 1.49 % at 1000 °C. But, the initial thermal loss (below 400 °C) was 0.62 %. The initial thermal loss usually happens due to the evaporation of absorbed water from the environment. Beyond that, further weight loss is associated with the valence changes of B-site cations and the formation of oxygen vacancies.

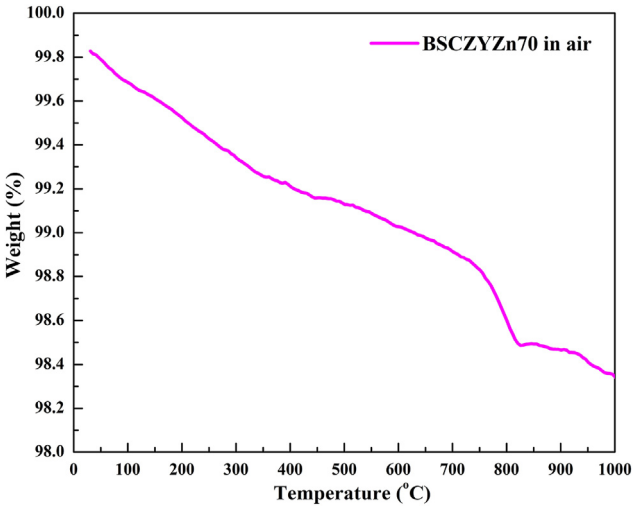

Fig. 4. Thermal behavior of BSCZYZn70 in air.

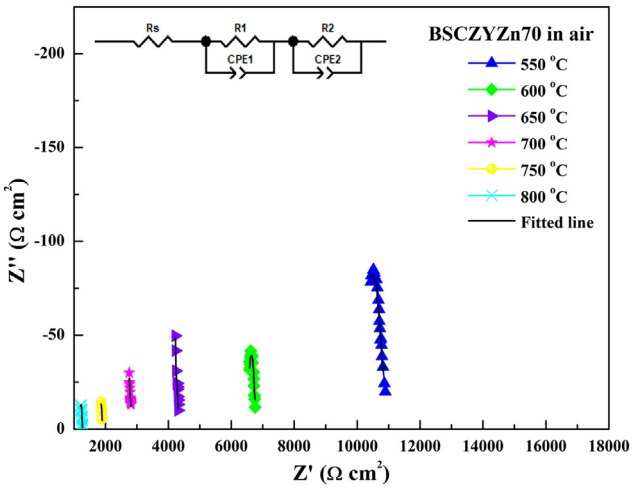

Fig. 5. Nyquist plots of impedance spectra of BSCZYZn70 in air and the equivalent circuit of EIS analyses are inserted in the figure.

3.4. Impedance analysis

Protons are considered to move by following the Grotthuss mechanism in proton-conducting perovskites [24,25]. It admits proton attachment to oxygen, reorientation influenced by nearby oxygen atoms, and subsequent transfer between oxygen sites, especially at high temperatures [6]. The choice of dopant significantly affects binding energy between hydroxyl radicals and dopant ions, with computational models—validated by experimental data—showing stronger, more stable interactions (more negative binding energies) for certain dopants like indium compared to yttrium or ytterbium [26]. However, the electrochemical properties of a material are critical for assessing its potential in fuel cell applications. To evaluate these properties of this study, impedance spectroscopy was executed in air atmosphere across a temperature range of 500–800 °C. This technique effectively measures a material's resistance and conductivity under varying conditions, as lower impedance corresponds to higher ionic conductivity. High proton conductivity, indicated by low impedance, is essential for efficient fuel cell operation. Thus, material demonstrating low impedance in the experiment is considered strong candidates for fuel cell application. Fig. 5 describes the impedance spectra of BSCZYZn70 in air. Resistance was obtained through fitting impedance data to a 3RC equivalent circuit model comprising resistors and parallel constant phase elements. For determining the conductivity and activation energy of BSCZYZn70, the following formula [9] is used,

$$\sigma = L/RA = \sigma_o e^{-E_a/RT} \quad (1)$$

Where, σ, L, R, A, σ_o, E_a, R, and T represent conductivity, length, resistance, area, pre-exponential factor, activation energy, gas constant, and temperature, respectively.

At 700 °C, the measured conductivity of BSCZYZn70 in air, was 1.056×10^{-4} Scm^{-1}, as described by Fig. 6. This result can be compared to the previous study [9], measured at dry H_2 atmosphere. It is notable that conductivity increases with rising temperature, as the thermal energy enhances atomic vibrations and promotes ion transport, thereby improving conductive performance. The measured (500–700 °C) activation energy (as listed in Table 3) of BSCZYZn70 in air was 0.60 eV. Activation energy measurements play a crucial role in understanding electrolyte behavior, as they

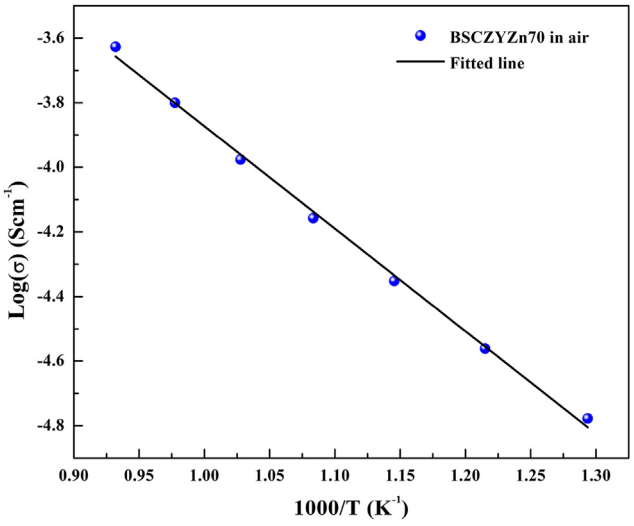

Fig. 6. Arrhenius plots of total conductivity of BSCZYZn70 in air.

Table 3. Conductivity and activation energy of BSCZYZn70 with other similar sample.

Sample	Conductivity (Scm^{-1})		Activation energy (eV)	Reference
	500 °C	700 °C	500 °C–700 °C	
	Air	Air	Air	
BSCZYZn70	1.669×10^{-5}	1.056×10^{-4}	0.60	This work
BSCZYZn30	9.76×10^{-5} (dry H_2)	8.99×10^{-4} (dry H_2)	0.733 (dry H_2)	[9]

reveal key information about energy barriers, ion transport mechanisms, and overall ionic conductivity. A lower activation energy suggests that ions can move more easily through the electrolyte, encountering minimal resistance, which leads to higher ionic conductivity. Conversely, an elevated activation energy indicates greater resistance to ion movement and larger energy barriers, resulting in reduced ionic conductivity. These insights are essential for evaluating and optimizing materials for IT-SOFC [27].

4. Conclusion

The perovskite-type material $Ba_{0.3}Sr_{0.7}Ce_{0.7}Zr_{0.1}Y_{0.15}Zn_{0.05}O_{3-\delta}$ showed cubic symmetry and *Pm-3m* space group by the Rietveld method. The material demonstrated advantageous grain growth, with the amalgamation of large and small grains, and achieved a relative density exceeding 99 %. This high relative density is crucial for electrolyte applications where high density and leak-tightness are essential. In addition, BSCZYZn70 demonstrated high thermal stability with a minimal thermal weight loss of only 1.49 %. Its low activation energy of 0.60 eV suggests enhanced ion transport properties, which is highly advantageous for proton-conducting electrolyte. These combined properties indicate that BSCZYZn70 is a promising candidate for use as an electrolyte in IT-SOFC. Further investigations, including testing under wet and dry H_2 atmospheres and performance evaluation in operating fuel cell, are planned for the future to fully assess its proton-conducting behavior.

Funding

No funding.

Conflicts of interest

No conflict of interest.

Acknowledgements

Md. Mosfiqur Rahman gratefully acknowledges the support provided by the UBD Graduate Scholarship. He also extends his sincere thanks to the Fuel Cell Institute, Universiti Kebangsaan Malaysia (UKM), and the School of Physics, Harbin Institute of Technology (HIT), China, for the valuable laboratory support.

References

[1] B. Wang, M. Liu, Z. Wu, X. Liu, M. Li, D. Tang, Effect of thermophysical properties of perovskite electrolytes on intermediate temperature SOFC, Int. J. Heat Mass Tran. 244 (2025) 126944, https://doi.org/10.1016/j.ijheatmasstransfer.2025.126944.

[2] M.M. Rahman, A.M. Abdalla, L.A. Omeiza, V. Raj, S. Afroze, M.S. Reza, A.K. Azad, Numerical modeling of ammonia-fueled protonic-ion conducting electrolyte-supported solid oxide fuel cell (H-SOFC): a brief review, Processes 11 (9) (2023) 2728, https://doi.org/10.3390/pr11092728.

[3] N. Radenahmad, A. Afif, M.I. Petra, S.M.H. Rahman, S. Eriksson, A. K. Azad, High conductivity and high density proton conducting Ba1− xSrxCe0. 5Zr0. 35Y0. 1Sm0. 05O3− δ (x= 0.5, 0.7, 0.9, 1.0) perovskites for IT-SOFC, Int. J. Hydrogen Energy 41 (27) (2016) 11832–11841, https://doi.org/10.1016/j.ijhydene.2016.02.073.

[4] A.K. Yadav, S. Sinha, A. Kumar, Advancements in composite cathodes for intermediate-temperature solid oxide fuel cells: a comprehensive review, Int. J. Hydrogen Energy 59 (2024) 1080–1093, https://doi.org/10.1016/j.ijhydene.2024.02.124.

[5] L.A. Omeiza, M.M. Rahman, K.A. Kuterbekov, A. Kabyshev, K. Bekmyrza, M. Kubenova, A.K. Azad, Novel sr-doped NdMn0. 5Cr0. 5O3-δ electrodes for symmetrical solid oxide fuel cell, Electrochem. Commun. 164 (2024) 107730, https://doi.org/10.1016/j.elecom.2024.107730.

[6] Z. Shi, W. Sun, W. Liu, Synthesis and characterization of BaZr0. 3Ce0. 5Y0. 2− xYbxO3− δ proton conductor for solid oxide fuel cells, J. Power Sources 245 (2014) 953–957, https://doi.org/10.1016/j.jpowsour.2013.07.060.

[7] A.K. Azad, A. Kruth, J.T. Irvine, Influence of atmosphere on redox structure of BaCe0. 9Y0. 1O2. 95—Insight from neutron diffraction study, Int. J. Hydrogen Energy 39 (24) (2014) 12804–12811, https://doi.org/10.1016/j.ijhydene.2014.05.080.

[8] S. Yu, J. Zhang, Y. Ma, J. Sun, L. Zhu, Electrical properties of an A-site Ba-doped LSGM ceramic electrolyte for IT-SOFC, Ceram. Int. (2025), https://doi.org/10.1016/j.ceramint.2025.02.030.

[9] M.M. Rahman, M. Ali, A. Hanjala, M.S. Khaled, A.M. Abdalla, L.A. Omeiza, A.K. Azad, Sr-doped BaCe0. 7Zr0. 1Y0. 15 Zn0. 05O3− δ electrolytes for intermediate temperature solid oxide fuel cell, J Solid State Electrochem (2025) 1–14, https://doi.org/10.1007/s10008-025-06252-x.

[10] M.M. Rahman, A.M. Abdalla, L.A. Omeiza, V. Raj, M.T. Le, B. Wei, A.K. Azad, Highly dense and thermally stable BaCe0. 5Zr0. 3Y0. 1A0. 05 Zn0. 05O3− δ (A= Gd, Sm) electrolyte for intermediate temperature solid oxide fuel cell (IT-SOFC), Ionics (2025) 1–12, https://doi.org/10.1007/s11581-024-06058-3.

[11] A. Sharma, K. Watanabe, H. Shimada, M. Jeem, Y. Yamaguchi, K. Nomura, M. Fujioka, Enhanced PCFC performance via anode additive BaCO3—Induced grain growth in BZYb electrolyte, J. Power Sources 631 (2025) 236198, https://doi.org/10.1016/j.jpowsour.2025.236198.

[12] L. Hamze, A.L.G. La Salle, O. Joubert, E. Quarez, Impact of sintering procedures on the densification and conductivity of BaZr0. 4Ce0. 4Y0. 1Yb0. 1O3-δ electrolyte for protonic ceramic fuel cells, Int. J. Hydrogen Energy 139 (2025) 316–324, https://doi.org/10.1016/j.ijhydene.2025.05.241.

[13] A. Afif, N. Radenahmad, S.M.H. Rahman, N. Torino, M. Saqib, S. Hossain, A.K. Azad, Ceramic fuel cells using novel proton-conducting BaCe 0.5 Zr 0.3 Y 0.1 Yb 0.05 Zn 0.05 O 3-δ electrolyte, J. Solid State Electrochem. (2022) 1—10, https://doi.org/10.1007/s10008-021-05062-1.
[14] Z. Shi, Y. Liu, J. Chen, Q. Zhao, H. Yang, S. Li, C. Chen, Electrolyte evolution: the impact of indium doping on BaCe0. 9Gd0. 1O3-δ, Int. J. Hydrogen Energy 126 (2025) 468—475, https://doi.org/10.1016/j.ijhydene.2025.04.033.
[15] S. Kalaimathi, K.S. Babu, A. Imtiyaz, Influence of fluorine doping on the electrical and optical properties of La0. 9Sr0. 1Ga0. 8Mg0. 2O3-δ solid electrolyte, J. Mater. Sci. Mater. Electron. 36 (6) (2025) 399, https://doi.org/10.1007/s10854-025-14473-z.
[16] E. Fabbri, A. D'Epifanio, E. Di Bartolomeo, S. Licoccia, E. Traversa, Tailoring the chemical stability of Ba (Ce0. 8− xZrx) Y0. 2O3−δ protonic conductors for intermediate temperature solid oxide fuel cells (IT-SOFCs), Solid State Ionics 179 (15—16) (2008) 558—564, https://doi.org/10.1016/j.ssi.2008.04.002.
[17] J. Rodríguez-Carvajal, Recent advances in magnetic structure determination by neutron powder diffraction, Phys. B Condens. Matter. 192 (1—2) (1993) 55—69, https://doi.org/10.1016/0921-4526(93)90108-I.
[18] J. Wu, R.A. Davies, M.S. Islam, S.M. Haile, Atomistic study of doped BaCeO3: dopant site-selectivity and cation non-stoichiometry, Chem. Mater. 17 (4) (2005) 846—851, https://doi.org/10.1021/cm048763z.
[19] R.L. Moreira, A. Dias, Comment on "Prediction of lattice constant in cubic perovskites", J Phys Chem Solid 68 (8) (2007) 1617—1622, https://doi.org/10.1016/j.jpcs.2007.03.050.
[20] K. Katahira, Y. Kohchi, T. Shimura, H. Iwahara, Protonic conduction in Zr-substituted BaCeO3, Solid State Ionics 138 (1—2) (2000) 91—98, https://doi.org/10.1016/S0167-2738(00)00777-3.
[21] P.K. Prajapati, D. Chaira, Fabrication and characterization of Cu—B 4 C metal matrix composite by powder metallurgy: effect of B 4 C on microstructure, mechanical properties and electrical conductivity, Trans. Indian Inst. Met. 72 (2019) 673—684, https://doi.org/10.1007/s12666-018-1518-2.
[22] Y. Lu, M.Y. Shah, N. Mushtaq, M. Yousaf, N. Akbar, N. Arshad, S. Irshad, An innovative perovskite oxide enabling improved efficiency for low-temperature ceramic electrochemical cells, Fuel 367 (2024) 131558, https://doi.org/10.1016/j.fuel.2024.131558.
[23] J. Gao, K. Chen, M. Akbar, C. Xia, W. Dong, X. Wang, B. Wang, Development of high-performance perovskite La (Mg2/3Nb1/3) O3 electrolyte with hybrid protonic/oxide ion conduction for low-temperature solid oxide fuel cells, Int. J. Hydrogen Energy 50 (2024) 361—373, https://doi.org/10.1016/j.ijhydene.2023.08.172.
[24] N. Agmon, The grotthuss mechanism, Chem. Phys. Lett. 244 (5—6) (1995) 456—462, https://doi.org/10.1016/0009-2614(95)00905-J.
[25] D. Marx, Proton transfer 200 years after von Grotthuss: insights from ab initio simulations, ChemPhysChem 7 (9) (2006) 1848—1870, https://doi.org/10.1002/cphc.200600128.
[26] M.S. Islam, P.R. Slater, J.R. Tolchard, T. Dinges, Doping and defect association in AZrO 3 (A= Ca, Ba) and LaMO 3 (M= Sc, Ga) perovskite-type ionic conductors, Dalton. Trans. (19) (2004) 3061—3066, https://doi.org/10.1039/b402669c.
[27] M.M. Rahman, L.A. Omeiza, A.M. Abdalla, V. Raj, M.T. Le, B. Wei, A.K. Azad, Gd, Sm, and Yb Co-doped proton-conducting electrolytes for an intermediate-temperature solid oxide fuel cell, J. Electron. Mater. (2025) 1—12, https://doi.org/10.1007/s11664-025-11959-8.
[28] S. Hossain, A.M. Abdalla, N. Radenahmad, A.K.M. Zakaria, J.H. Zaini, S.H. Rahman, A.K. Azad, Highly dense and chemically stable proton conducting electrolyte sintered at 1200 C, Int. J. Hydrogen Energy 43 (2) (2018) 894—907, https://doi.org/10.1016/j.ijhydene.2017.11.111.
[29] S. Hossain, A.M. Abdalla, J.H. Zaini, C.D. Savaniu, J.T. Irvine, A.K. Azad, Highly dense and novel proton conducting materials for SOFC electrolyte, Int. J. Hydrogen Energy 42 (44) (2017) 27308—27322, https://doi.org/10.1016/j.ijhydene.2017.09.067.